Pacific Northwest
NATIONAL LABORATORY

PNNL-33457

# Synthesis and Photonic Sintering of Proton Conducting Lanthanide Nickelates

September 2022

Brent W Kirby
Katarzyna Grubel
Ewa C Ronnebro
John S Hardy
Junyoung Kim

U.S. DEPARTMENT OF ENERGY

Prepared for the U.S. Department of Energy
under Contract DE-AC05-76RL01830

## DISCLAIMER



PACIFIC NORTHWEST NATIONAL LABORATORY
*operated by*
BATTELLE
*for the*
UNITED STATES DEPARTMENT OF ENERGY
*under Contract DE-AC05-76RL01830*

**Printed in the United States of America**

**Available to DOE and DOE contractors from the Office of Scientific and Technical Information,**
**P.O. Box 62, Oak Ridge, TN 37831-0062**
www.osti.gov
**ph: (865) 576-8401**
**fax: (865) 576-5728**
**email: reports@osti.gov**

**Available to the public from the National Technical Information Service**
**5301 Shawnee Rd., Alexandria, VA 22312**
**ph: (800) 553-NTIS (6847)**
**or (703) 605-6000**
**email: info@ntis.gov**
**Online ordering: http://www.ntis.gov**

PNNL-33457

# Synthesis and Photonic Sintering of Proton Conducting Lanthanide Nickelates

September 2022

Brent W Kirby
Katarzyna Grubel
Ewa C Ronnebro
John S Hardy
Junyoung Kim

Prepared for
the U.S. Department of Energy
under Contract DE-AC05-76RL01830

Pacific Northwest National Laboratory
Richland, Washington 99354

# Abstract

Lanthanide nickelate perovskites are known proton conductors at intermediate temperatures (350-600°C). They are attractive targets for proton conducting fuel cells and electrolyzers due to their operational temperature range and their stability in the presence of $CO_2$. These materials have the formula $LNiO_3$, with the lanthanide L = La, Ce, Pr, Nd, or Sm. Sintering is challenging due to phase transformations that occur at lower temperatures than those required for sintering. In this project, a series of lanthanide nickelate perovskites was synthesized via both a precursor solid solution method and the glycine nitrate process.

Powders derived from the precursor solid solution method for $LaNiO_3$ and $NdNiO_3$ were sintered at Utility Global Inc. at various temperatures utilizing fast photonic sintering. $LaNiO_3$ was successfully sintered while maintaining the perovskite phase. $NdNiO_3$ underwent a phase transformation at all the conditions tested. The stability of the perovskite phase decreases moving right across the lanthanides in the periodic table, while the expected proton conductivity increases. These results will inform further investigations into lanthanide nickelate perovskites toward the goal of producing a free-standing, sintered, proton-conducting membrane.

# Acknowledgments

This research was supported by the Energy and Environment Mission Seed Initiative, under the Laboratory Directed Research and Development (LDRD) Program at Pacific Northwest National Laboratory (PNNL). PNNL is a multi-program national laboratory operated for the U.S. Department of Energy (DOE) by Battelle Memorial Institute under Contract No. DE-AC05-76RL01830.

The authors would also like to acknowledge David Leu of Utility Global, Inc. for performing sintering experiments and SEM analysis.

# Contents



# Figures

## Tables

# 1.0 Introduction

Lanthanide nickelate perovskites are known proton conductors at intermediate temperatures (350-600°C). They are attractive targets for proton conducting fuel cells and electrolyzers due to their operational temperature range and their stability in the presence of $CO_2$. These materials have the formula $LNiO_3$, with the lanthanide L = La, Ce, Pr, Nd, or Sm. Sintering is challenging due to phase transformations that occur at lower temperatures than those required for sintering.

These materials have been studied previously at PNNL under the Quickstarter funding program. Under that program, $NdNiO_3$ was synthesized via a solid solution precursor of hydroxides formed using bubbled chlorine gas. The powder was processed into an ink at Utility Global, Inc. and sintered onto a NiO/YSZ (yttria stabilized zirconia) substrate using fast photonic sintering. Sintering attempts either were too aggressive, resulting in a phase change of the material, or not aggressive enough, resulting in no sintering activity.

This work developed a more benign solution-based synthesis method for lanthanide nickelate perovskites, as well as exploring the possibility of using the glycine nitrate process to yield finer particles. Two primary lanthanides were studied, La and Nd. The stability of the perovskite phase decreases moving right across the lanthanides in the periodic table, while the expected proton conductivity increases. La and Nd effectively bracket the range of properties across the lanthanides.

A targeted range of photonic sintering conditions were attempted at Utility Global, Inc. with single layers of ink from a given powder deposited on an NiO/YSZ substrate, as in previous experiments. $LaNiO_3$ was successfully sintered while maintaining the perovskite phase. $NdNiO_3$ underwent a phase transformation at all the conditions tested, and may not be stable enough to sinter in air, even at very short heating durations.

# 2.0 Synthesis

## 2.1 Precursor Solid Solution Method

The first trials during the Quickstarter project to make $NdNiO_3$ used a precursor solid solution synthesis route (Vidyasagar et al, 1985) involving hydroxide solid solutions of metal nitrates saturated with chlorine gas that were filtered, washed and dried. Using chlorine gas is hazardous and we therefore explored other more benign synthesis routes.

A summary of solution-based syntheses, including previous work from the Quickstarter program (designated QS) are presented in Table 1. Despite the apparent wealth of synthetic procedures, pure materials were not obtained by any method attempted, including a gelatin method (Oliveira et al., 2013) and a citric acid method (Le et al., 2006). Therefore, the procedure outlined by Vidyasagar was modified. In this modification, instead of preparing hypochlorite in situ with bubbling chlorine gas, commercially available concentrated Clorox® bleach is utilized. The general procedure for this synthesis is as follows.

Equimolar amounts of Nd and Ni nitrate salts were mixed together in 10 mL of distilled water and stirred until everything dissolved. To such solution, about 50 mL of bleach was added until reaction turned dark brown, and a precipitate formed. At this point, the reaction was alkalized to pH 12 with solid NaOH and left stirring overnight at ambient temperature. After this time, the reaction was filtered through a medium frit and the obtained precipitate was washed on the filter with DI water until the pH of the filtrate was 7. The precipitate was then collected and dried for 12 h at 120 °C with a heating rate of 10 °C/min. Obtained black crystalline material was ground until it was fine and powdery and annealed at either 650 °C for 12 h under flow of pure $O_2$ with a heating rate 5 °C/min.; or 700 °C for 12 h in air with a heating rate 10 °C/min. XRD (x-ray diffraction) analysis indicated purity of about 70%, with 30% of formed NiO. This result prompted an adjustment in the stoichiometry of initial materials to 1:1.3 nickel:lanthanide. The rest of the synthesis was carried out as described.

Table 1. Summary of PNNL synthesis and XRD analysis of lanthanide nickelates.

| Sample ID | Synthesis date | Mixed Oxide | Synthesis route | Reference | XRD phase analysis |
|---|---|---|---|---|---|
| QS | | $NdNiO_3$ | Chlorine gas<br>Heat 600C, $O_2$ | Vidyasagar *et al*., 1985 | $NdNiO_3$ |
| QS | | $NdNiO_3$ | Chlorine gas<br>Heat 650C, air | Vidyasagar *et al*., 1985 | $NdNiO_3$ |
| QS | | $SmNiO_3$ | Chlorine gas<br>Heat 650C, air | Vidyasagar *et al*., 1985 | $Sm_2O_3$ |
| QS | | $SmNiO_3$ | Chlorine gas<br>Heat 900C, air | Vidyasagar *et al*., 1985 | $Sm_2O_3$, NiO |
| QS | | $NdNiO_3$ | Chlorine gas<br>Heat 1000C | Vidyasagar *et al*., 1985 | $Nd_2NiO_4$, $NdNiO_3$ |
| QS | | $NdNiO_3$ | Chlorine gas<br>Heat 650C, air | Vidyasagar *et al*., 1985 | $NdNiO_3$ |
| QS | | $NdNiO_3$ | Chlorine gas<br>Heat 950C, air | Vidyasagar *et al*., 1985 | $NdNiO_3$, 25% $Nd_2NiO_4$ |
| LDRD1 | 16Feb2022 | $NdNiO_3$ | Gelatin<br>Heat 905°C, 4h | Oliveira *et al.,* 2013 | $Nd_2NiO_4$, $Nd_4Ni_3O_{10}$, $Nd_2O_3$, $NdNiO_3$ |
| LDRD2 | 21Feb2022 | $LaNiO_3$ | Gelatin<br>Heat 900°C, 2h | Oliveira *et al.,* 2010 | $La_2O_3$ (10%), $La(OH)_3$ (10%) , NiO (5%), $LaNiO_3$ (70-75%). |
| LDRD3 | 4Mar2022 | $LaNiO_3$ | Citric acid<br>Heat 800°C,2 h | Le *et al.*, 2006 | LaNiO3, La2O3 |
| LDRD4 | 9Mar2022 | $LaNiO_3$ | Citric acid<br>Heat 800°C,2 h | Le *et al.*, 2006 | $La_2O_3$ (10%), $La(OH)_3$ (10%) , $NiO_2$ (5%), $LaNiO_3$ (70-75%) |
| LDRD5 | 31Mar2022 | $NdNiO_3$ | Bleach<br>Heat 650°C, $O_2$ | Based on Vidyasagar *et al.*, 1985 | Rietveld refinement of longscan: NdNiO3 (75%); NiO (25%). |
| LDRD6 | 31Mar2022 | $NdNiO_3$ | Bleach<br>Heat 700°C, air | Based on Vidyasagar *et al.*, 1985 | $NdNiO_3$ (75%); NiO (25%) LDRD5&6 similar per comparison<br>Sample sent to Utility Global for sintering, see Table 4 |
| LDRD7 | 16Mar2022 | $LaNiO_3$ | Bleach<br>Heat 750°C, 1.5h | Based on Vidyasagar *et al.*, 1985 | 80% $LaNiO_3$, ca20% NiO; Similar to LDRD5&6<br>Sample sent to Utility Global for sintering, see Table 4 |
| LDRD8 | 27Jun2022 | $NdNiO_3$ | Bleach<br>Heat 700°C, air | Based on Vidyasagar *et al.*, 1985 | Rietveld refinement of long scan: $NdNiO_3$ (76%), NiO amorphous (24%). |

## 2.2 Glycine Nitrate Method

Sintering activity is greater with smaller particle size. With that motivation, the glycine nitrate method (Chick, et al., 1990) was used to synthesize a range of lanthanide nickelates. The glycine nitrate process involves mixing a aqueous solution of metal nitrates in the appropriate stoichiometric ratio for the target material. Glycine is added in various ratios as a fuel for combustion. The solution is heated to drive off water, resulting in an increasingly viscous solution with an increasing boiling point. Eventually, the solution autoignites, leaving behind an ash of the ceramic material of interest. Uniformity is excellent due to molecular level mixing in the solution, and particle sizes are typically small.

The lanthanide nickelates $LNiO_3$ with L = La, Ce, Pr, and Nd were targeted using glycine/nitrate ratios of 1.2, 2.0, and 3.0. Higher glycine/nitrate ratios result in a lower temperature flame due to the fuel-rich conditions. The only material that formed the desired phase during glycine nitrate synthesis was $LaNiO_3$. This is the most stable lanthanide nickelate. Flame temperatures were likely too high to form the desired phase with the other lanthanides. Further details on XRD analysis are described in Section 4.1. None of these powders were submitted to sintering experiments due to the low quantity produced.

Table 2. Summary of glycine nitrate experiments and results.

| G/N ratio | $LaNiO_3$ | $CeNiO_3$ | $PrNiO_3$ | $NdNiO_3$ |
|---|---|---|---|---|
| **1.2** | N/A | $CeO_2$ + NiO rich phase | N/A | $Nd_2O_3$ + NiO rich phase |
| **2.0** | LaNiO3 rich phase (93%) | $CeO_2$ + NiO rich phase | $PrNiO_3$ (13%) +$Pr_2O_3$ + NiO rich phase | $Nd_2O_3$ + NiO rich phase |
| **3.0** | $LaNiO_3$ rich phase (99%) | $CeO_2$ + NiO rich phase | $PrNiO_3$ (16%) +$Pr_2O_3$ + NiO rich phase | $NdNiO_3$ (24%) + $Nd_2NiO_4$ (51%) rich phase |

# 3.0 Sintering Experiments

Powders (LDRD6 and LDRD7) were sent to Utility Global, Inc. for sintering experiments. Utility Global uses photonic sintering, where thin layers of material are rapidly heated by powerful lamps. Heating times are much less than one second, and the bulk of the material remains at a much lower temperature than the surface. Powdered materials are processing into inks, which are then sprayed onto a substrate in a thin layer, dried, and then photonically heated for sintering. Multiple layers can be added to build up a thicker final sample.

The temperature is monitored by optical instruments. If the emissivity of a material is known, a true temperature can be deduced. The emissivity of the lanthanide nickelates was not known for these experiments, so a nominal emissivity value was assumed. Thus, the “temperatures” described for these experiments are not true temperatures, but rather self-consistent proxies for temperature.

All samples described here were deposited on a NiO/YSZ substrate to mimic a solid oxide fuel cell configuration. The rapid surface heating method means that the substrate should have little interaction with the coating material. It does mean, however, that NiO and YSZ are apparent in the XRD phase analysis (see Section 4.2).

Previous experiments with $NdNiO_3$ during the Quickstarter project were performed in May and September of 2021. These results showed sintering as low as 1120°C with a phase change, and maintenance of the desired phase up to 910°C, but without sintering. One goal of the current project was to fill in the temperature range between these two results to look for conditions that would achieve both sintering and the maintenance of the desired phase. The full list of experimental conditions is shown in Table 2.

The first experiments for the current project involved three layers of material for both the Nd and La materials. This was done as a step toward a free standing membrane, as well as to have enough material for quality XRD data. However, temperature control proved more difficult for the three layer samples. The three peak temperatures listed in Table 2 for the three-layer samples represent the peak temperatures for each individual heating cycle on each individual layer. Since there was a specific temperature range of interest, the decision was made to focus only on single layers for subsequent experiments.

For $NdNiO_3$, the gap between 910°C and 1120°C was filled in with samples sintered at 940°C, 970°C, and 1040°C. All of those samples showed sintering activity (see Section 3.1), but also showed a phase change (see Section 4.2).

$LaNiO_3$ was expected to be somewhat more stable than $NdNiO_3$, and single-layer experimental temperatures were chosen accordingly at 970°C, 1045°C, and 1080°C. A preliminary three-layer sample was heated to peak temperatures of 1250/950/1050°C. This sample showed sintering activity, but also a phase change. However, the three single-layer samples all showed sintering activity while maintaining the desired $LaNiO_3$ phase.

Table 3. Experimental history of Utility Global, Inc. sintering experiments on lanthanide nickelates

| PNNL ID | Utility Global ID | Peak Sintering Temperature (~°C) | Sintered? | Maintain Phase? |
|---|---|---|---|---|
| QS | | 1120 | Yes | No |
| QS | | 1220 | Yes | No |
| QS | Ri | 740 | No | Yes |
| QS | Rii | 910 | No | Yes |
| QS | Riii | 605 | No | Yes |
| QS | Riv | 730 | No | Yes |
| LDRD 6 | NNi | 1250/950/1050 (three layers) | Yes | No |
| LDRD 6 | NNii | 1100/980/1080 (three layers) | Yes | No |
| LDRD 6 | NNiii | 940 | Yes | No |
| LDRD 6 | NNiv | 970 | Yes | No |
| LDRD 6 | NNv | 1040 | Yes | No |
| LDRD 6 | NN0 | Unsintered control | No | Yes |
| LDRD 7 | LNi | 1250/1155/1150 (three layers) | Yes | No |
| LDRD 7 | LNii | 970 | Yes | Yes |
| LDRD 7 | LNiii | 1045 | Yes | Yes |
| LDRD 7 | LNiv | 1080 | Yes | Yes |
| LDRD 7 | LN0 | Unsintered control | No | Yes |

## 3.1 SEM Analysis

SEM was performed on all sintered samples by Utility Global, Inc. Sintering activity, defined here as grain-to-grain bonding, was observed in all samples of the current work (NNi through NNv, and LNi through LNiv). Representative micrographs are presented in the Figures below.

Bright spots appear on the particles in many images. Analysis of these spots has not been done. It is likely a contaminant phase, possibly NiO from the powder synthesis. It could also be the undesirable $(La/Nd)_2NiO_4$ phase.

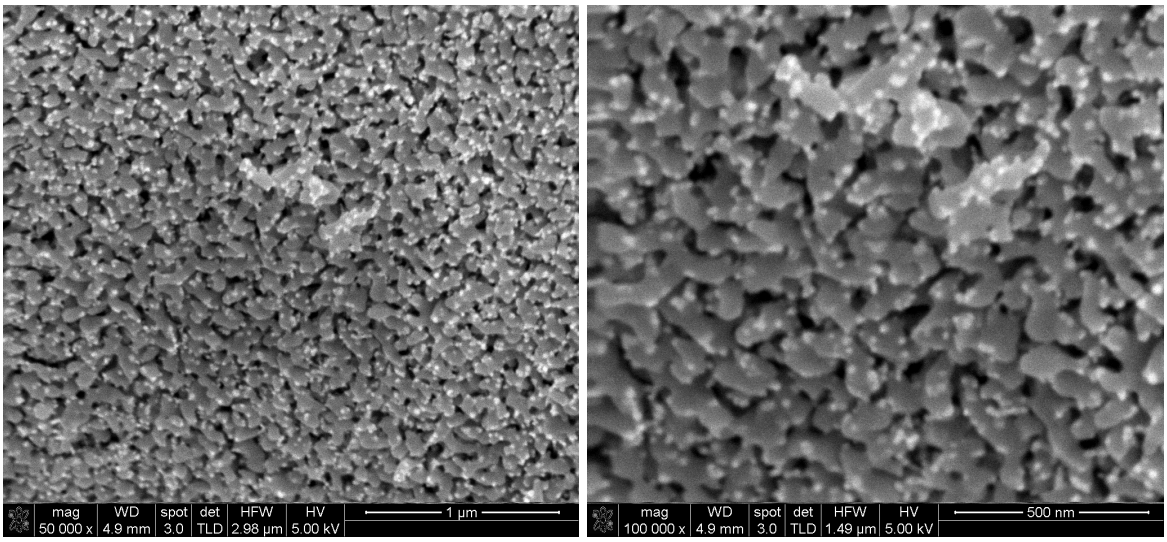


Figure 1. Sample NNi (three layers, 1250/950/1050°C) at 50,000 x and 100,000 x.

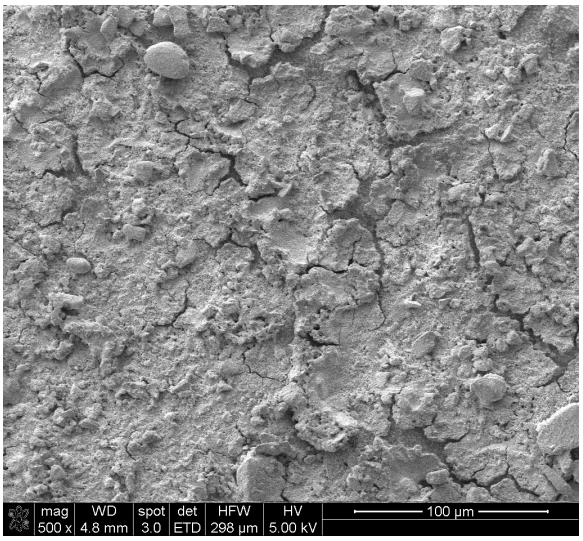


Figure 2. Sample NNii (three layers, 1100/980/1050°C) at 500 x.

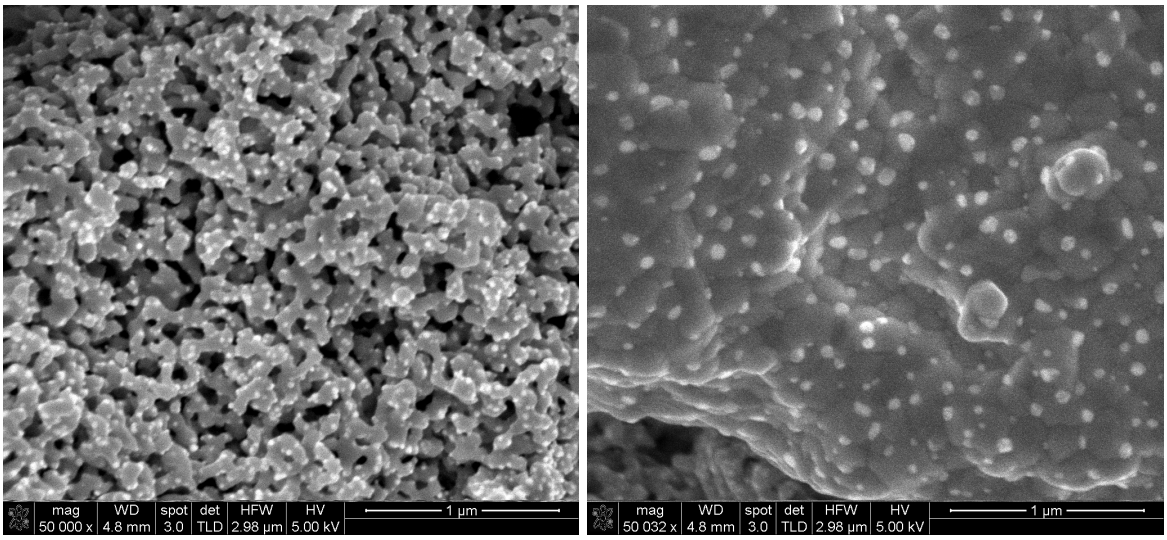


Figure 3. Two regions of sample NNii (three layers, 1100/980/1050°C) at 50,000 x.

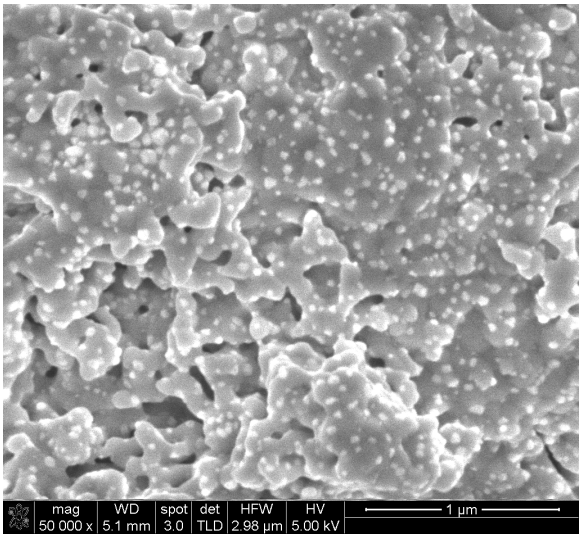


Figure 4. Sample NNiii (one layer, 940°C) at 50,000 x.

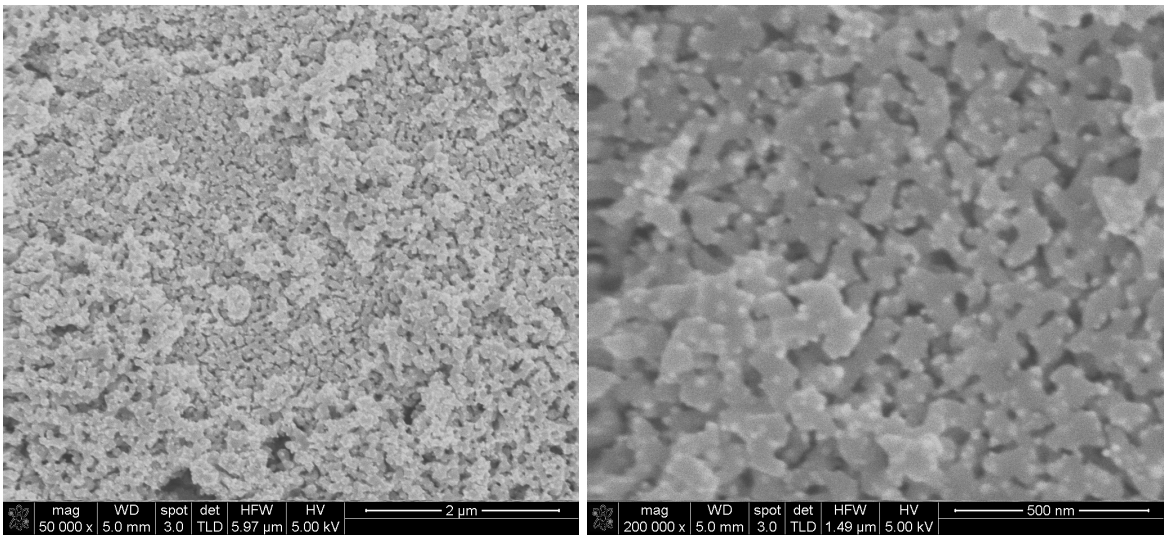


Figure 5. Sample NNiv (one layer, 970°C) at 50,000 x and 200,000 x.

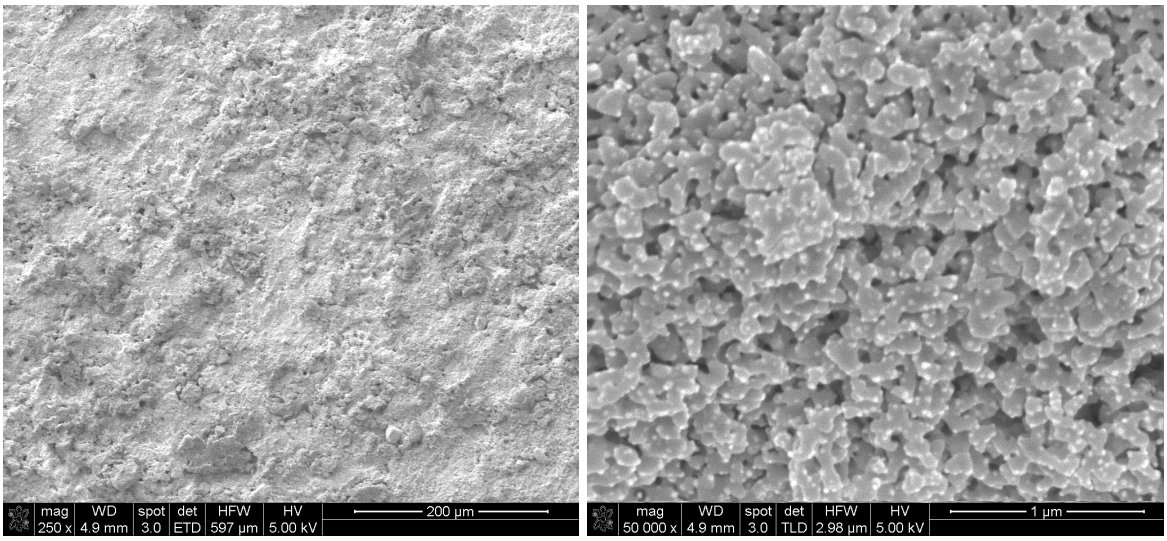


Figure 6. Sample NNv (one layer, 1040°C) at 250 x and 50,000 x.

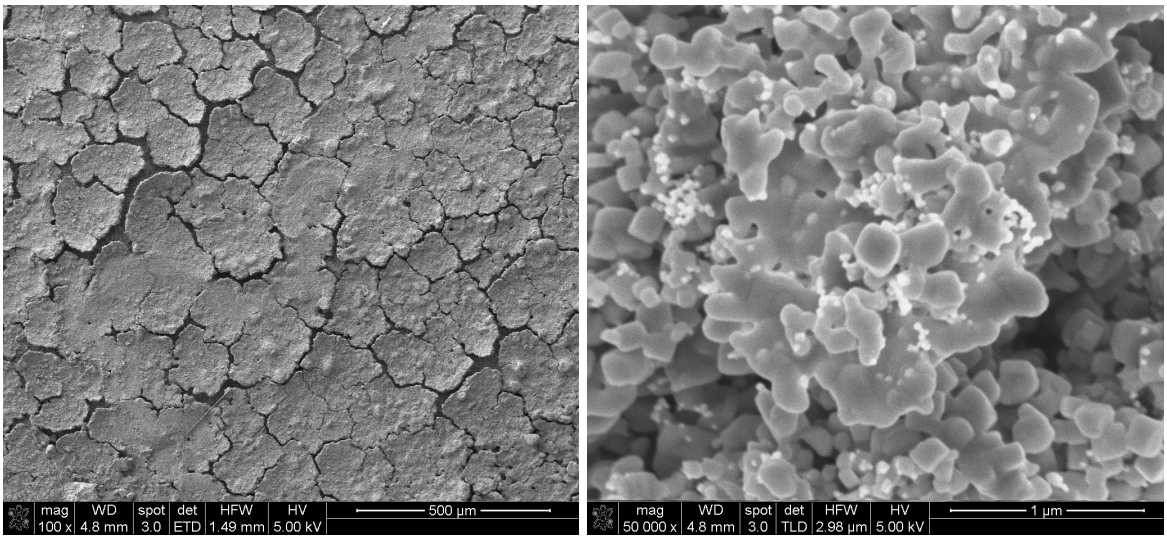


Figure 7. Sample LNi (three layers, 1250/1155/1150°C) at 100 x and 50,000 x.

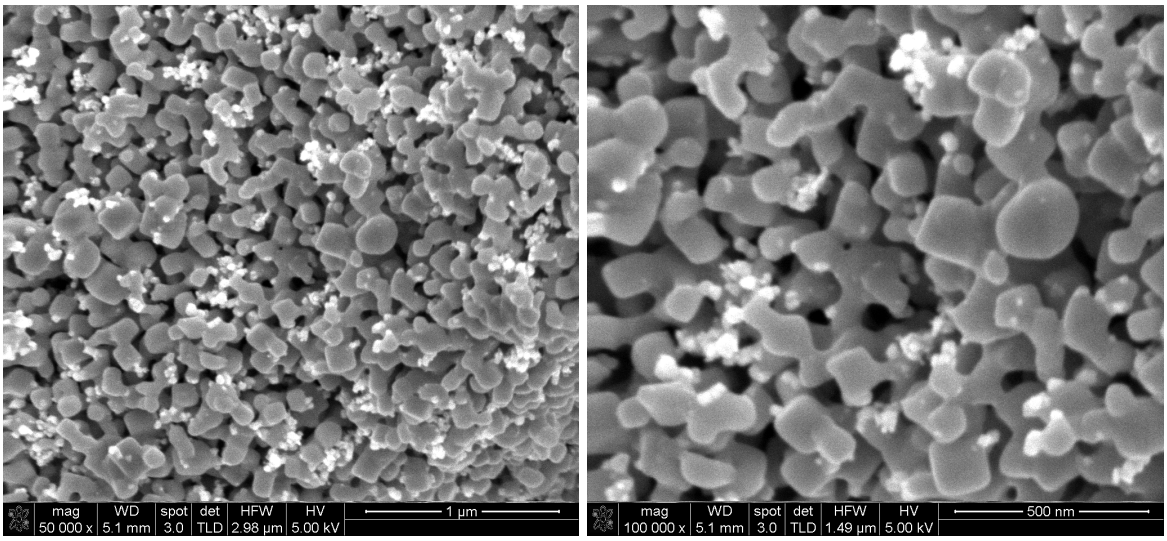


Figure 8. Sample LNii (one layer, 970°C) at 50,000 x and 100,000 x.

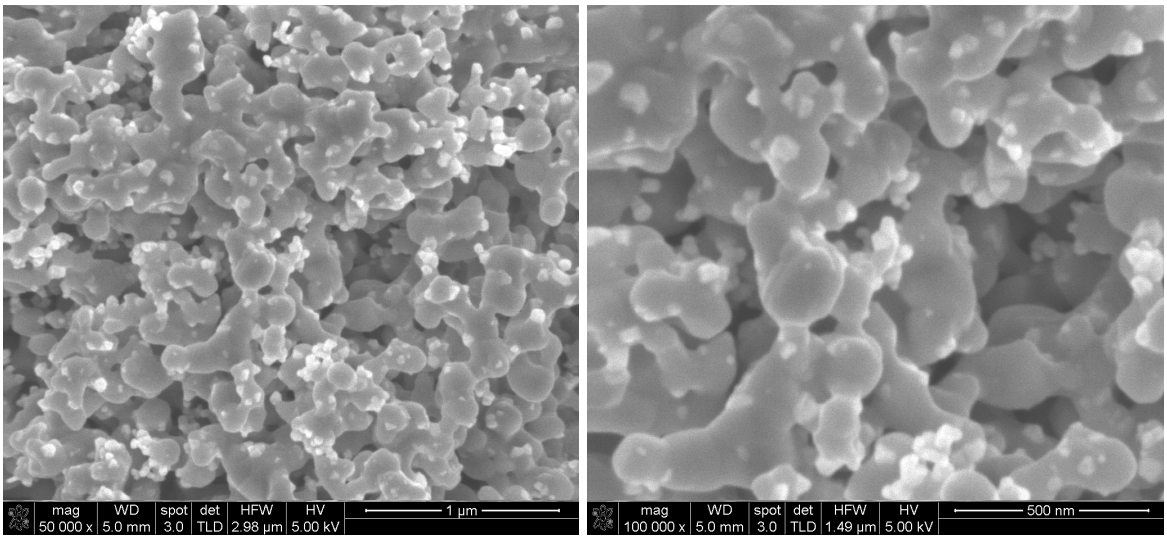


Figure 9. Sample LNiii (one layer, 1045°C) at 50,000 x and 100,000 x.

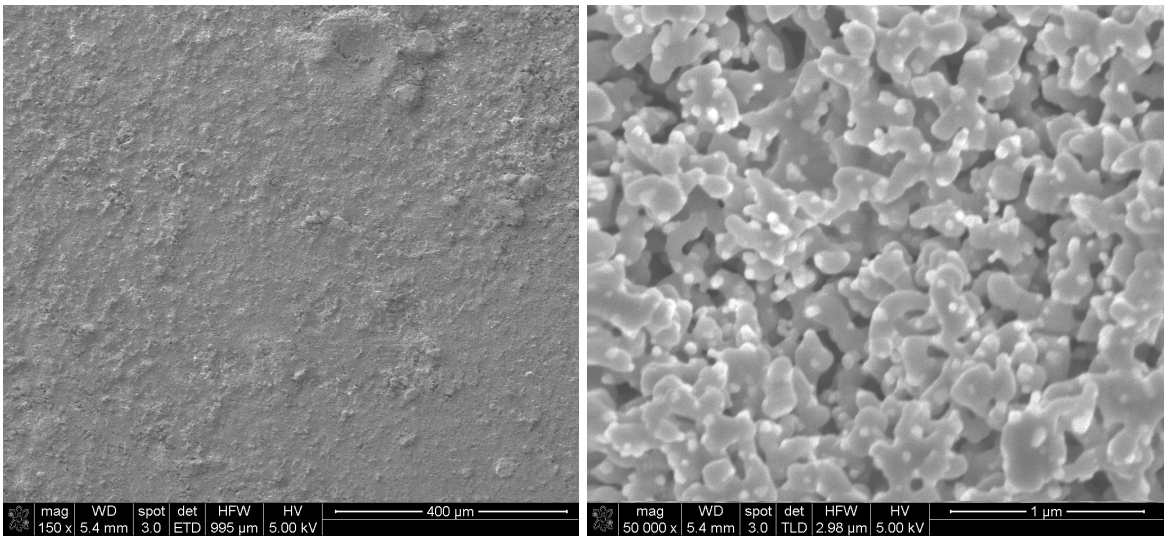


Figure 10. Sample LNiv (one layer, 1080°C) at 150 x and 50,000 x.

# 4.0 XRD Analysis

## 4.1 Glycine Nitrate Powders

Portions of the as-prepared powders from the glycine nitrate process were calcined at 700°C, 900°C, and 1100°C. All of these powders were submitted to XRD analysis for phase identification. These results are summarized in Figure 11 through Figure 14. A brief summary of all results is shown in Table 2.

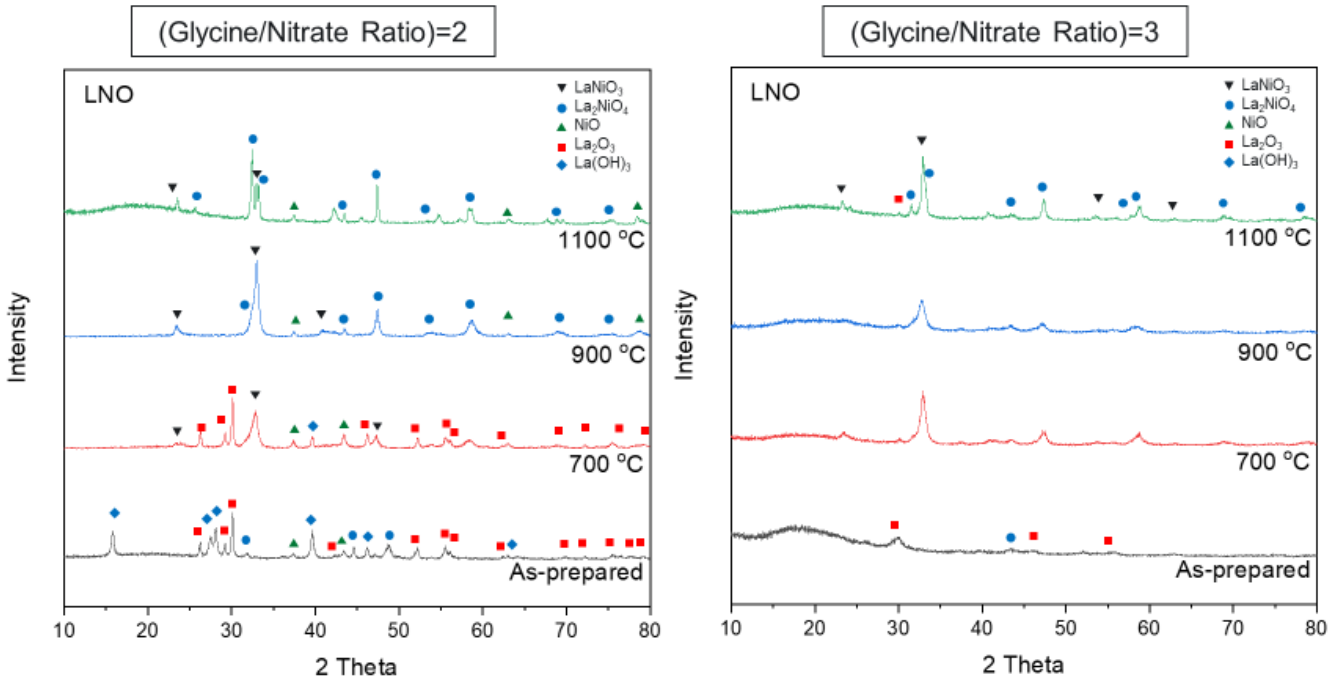


Figure 11. Glycine nitrate XRD results for $LaNiO_3$. The highest purity (99%) was achieved after sintering at 700°C.

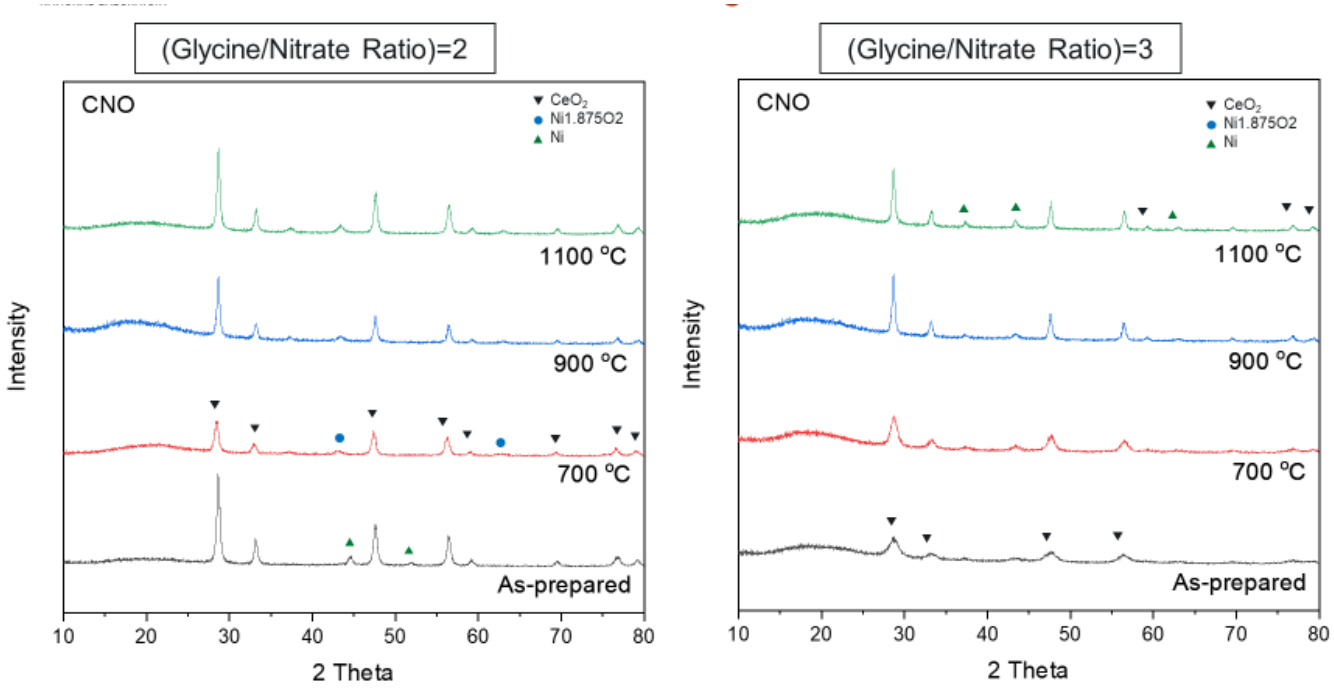


Figure 12. Glycine nitrate XRD results for $CeNiO_3$.

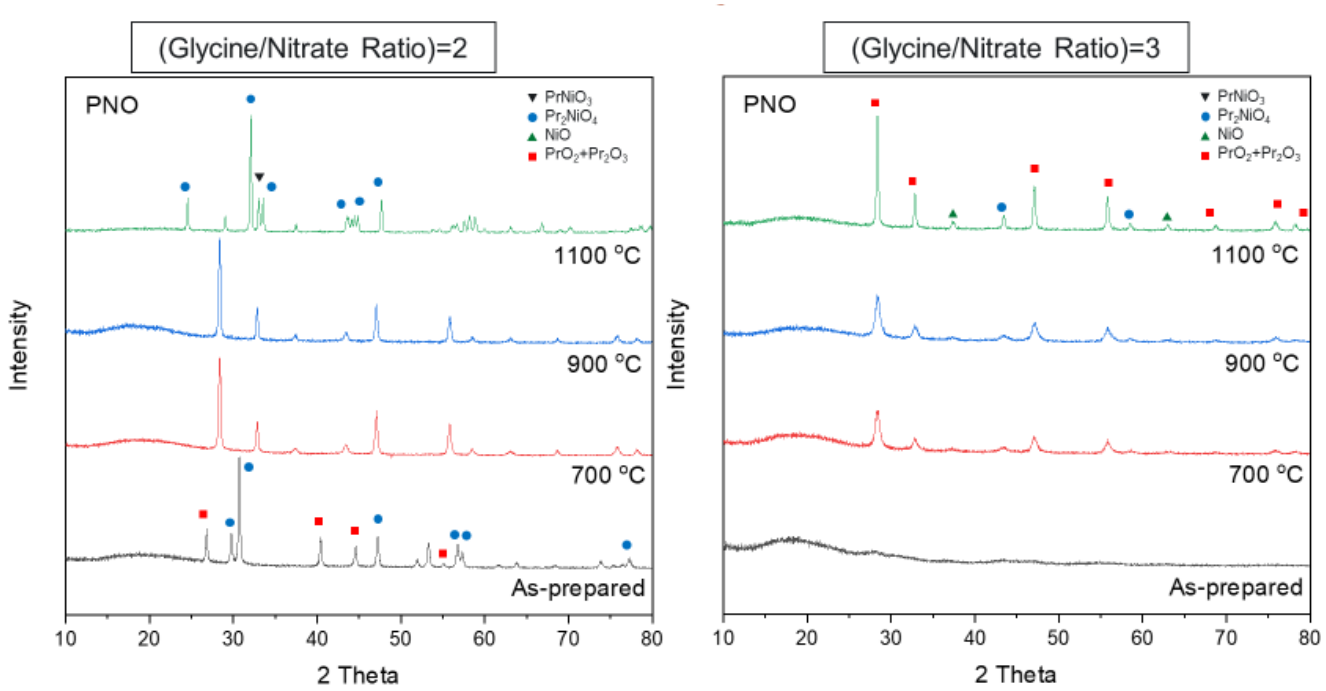


Figure 13. Glycine nitrate XRD results for $PrNiO_3$.

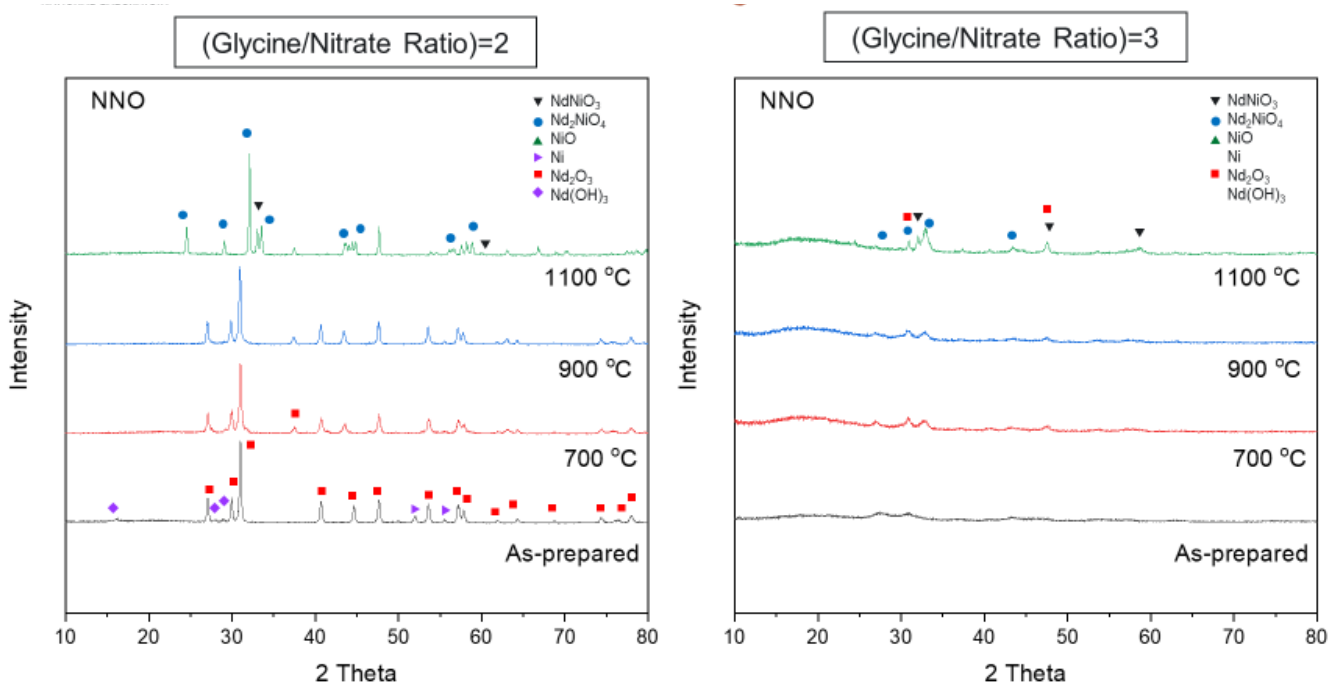


Figure 14. Glycine nitrate XRD results for $NdNiO_3$. The $Nd_2NiO_4$ phase becomes more stable as the calcination temperature increases.

## 4.2 Precursor Solid Solution Powders

To identify the phases, a benchtop Rigaku Mini-Flex powder XRD instrument was used. Rietveld refinement analysis was performed of selected samples to verify phase composition and phase contribution. To obtain data with sufficient counting statistics, XRD-patterns were collected at 10-100°, step 0.02°, dwell time 10 seconds per step. Figure 1 compares $NdNiO_3$ made by solid solution precursor route using chlorine with $NdNiO_3$ made using bleach and heat treated in both air and oxygen atmosphere, all three showing similar phase. Figure 2 compares $NdNiO_3$ made by bleach route and heat treated at 650C in oxygen (LDRD5) and 700C in air (LDRD6) and the patterns look similar. Data of LDRD5 was collected to obtain high counting statistics and Rietveld refinement confirmed formation of $NdNiO_3$ and 25% NiO. There is also an unknown amorphous phase present.

Figure 3 compares $NdNiO_3$ (LDRD6) and $LaNiO_3$ (LDRD7) both made by the bleach route. The XRD patterns look similar and can be indexed with the $NdNiO_3$ phase. Figure 4 compares $LaNiO_3$ samples; LDRD2 made by gelatin route, and LDRD3 & LDRD4 made by citric acid route. The gelatin and citric acid routes resulted in a product that contains hydroxides and oxides while the bleach route (LDRD7) resulted in a higher yield than similarly formed $NdNiO_3$.

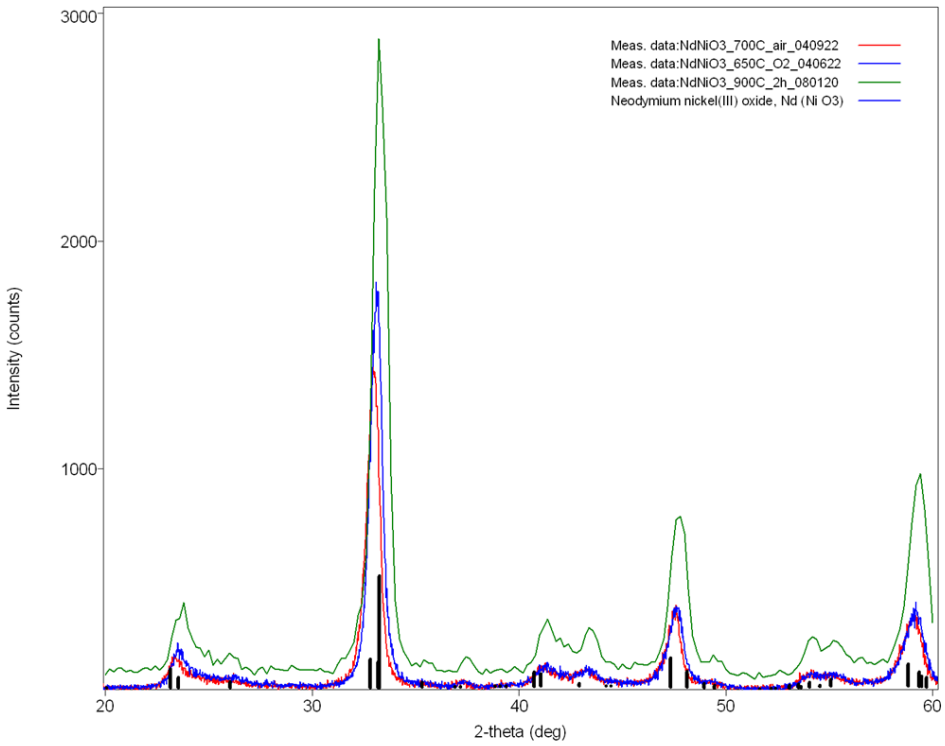


Figure 15. XRD patterns of $NdNiO_3$ made by using chlorine (green QS) or bleach (red LDRD6 and blue LDRD5).

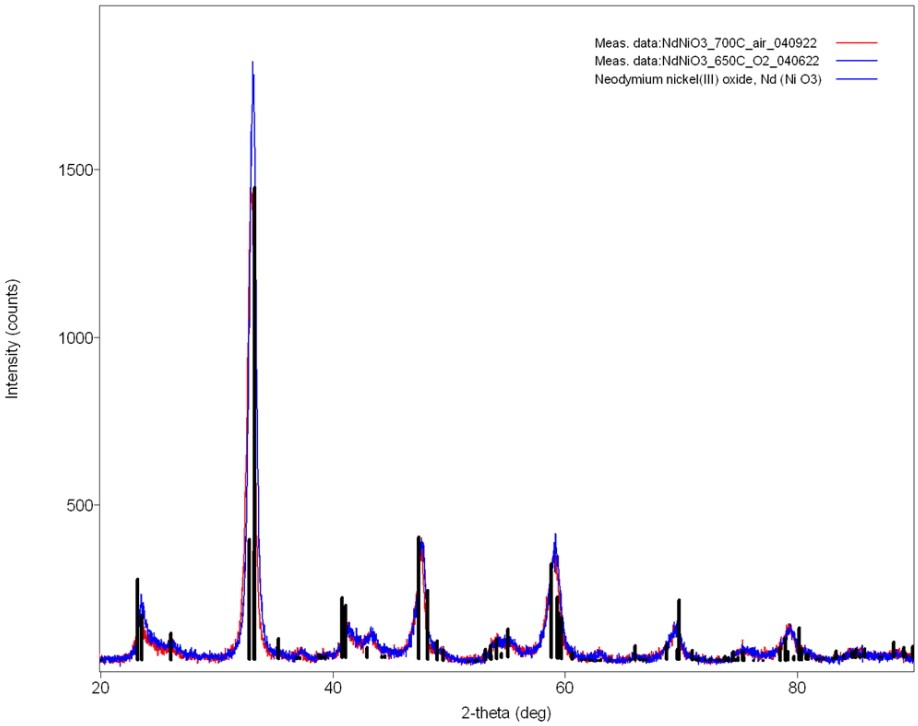


Figure 16. XRD-patterns of $NdNiO_3$ indexed with $NdNiO_3$ phase; heat treated at 700°C in air (red LDRD6) and heat treated at 650°C in oxygen (blue LDRD5).

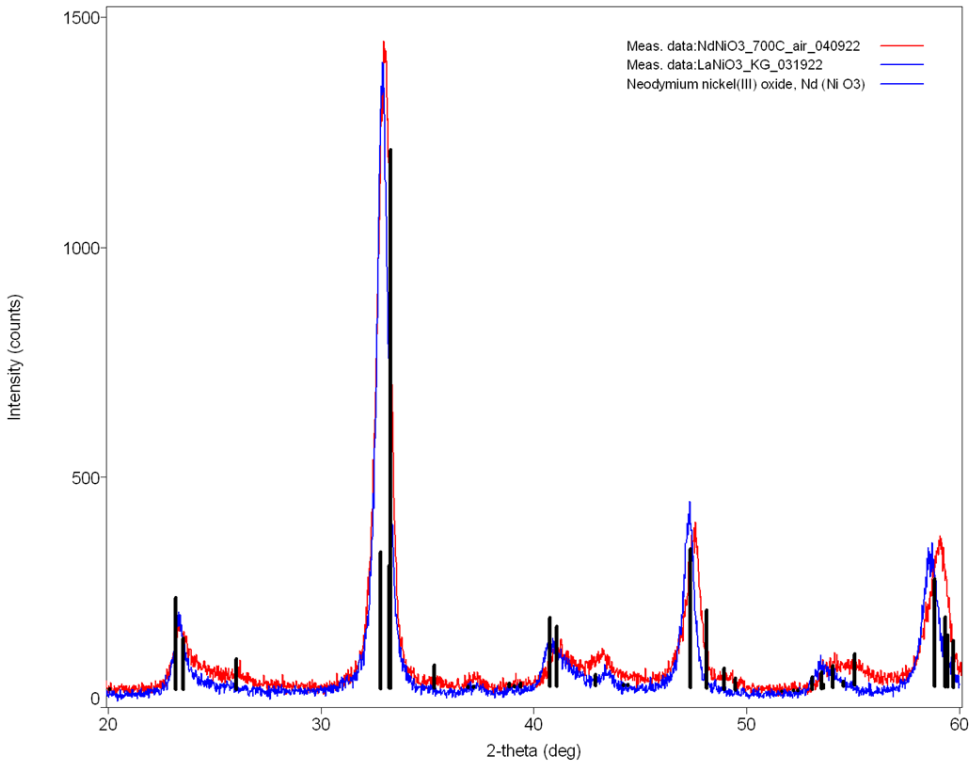


Figure 17. XRD patterns of $NdNiO_3$ heat treated at 700°C in air (red LDRD6) and $LaNiO_3$ (blue LDRD4). Indexed phase is $NdNiO_3$.

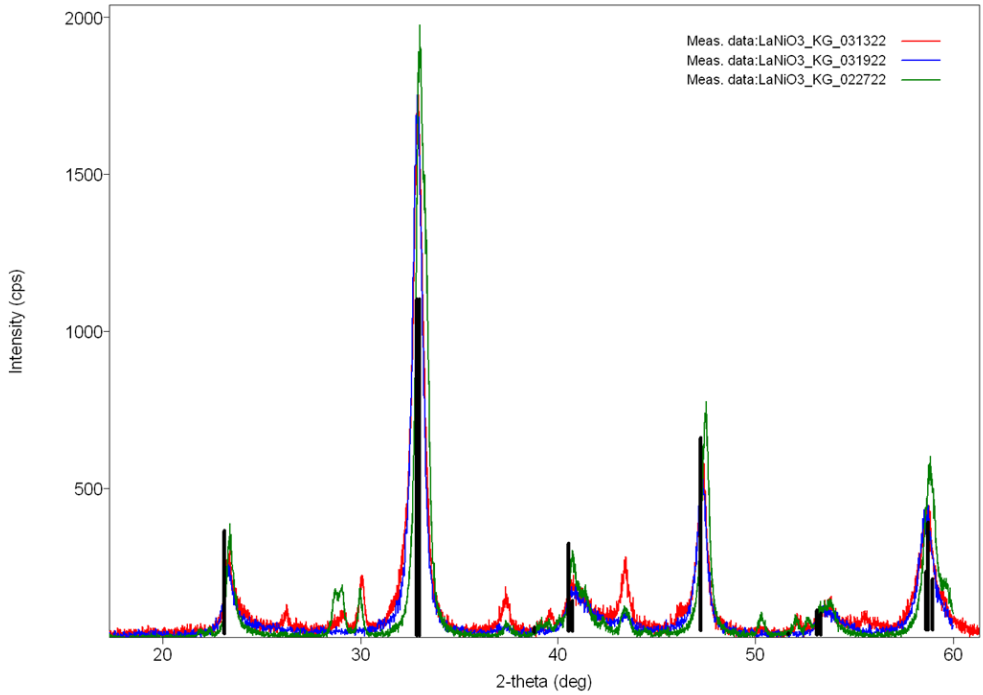


Figure 18. XRD patterns of $LaNiO_3$ made by gelatin route (green LDRD2) or citric acid route (red LDRD3 and blue LDRD4). The third trial (blue) has the highest yield (LDRD4).

## 4.3 Sintered Samples

To identify the phases after sintering, a benchtop Rigaku Mini-Flex powder XRD instrument was used. XRD-patterns were collected at 20-60°, step 0.2°, dwell time 2 seconds per step. The perovskite materials were applied as an ink on substrates of NiO/YSZ. Those substrates were mounted on SEM stubs for analysis at Utility Global, Inc. The SEM stubs were cut down so the specimens had a 1-2 mm thickness. By using a sample holder with a deep cavity, the specimen could become flush with the sample holder surface to collect relevant data. Results are tabulated in Table 2.

XRD patterns are presented in Figure 5 through Figure 10. It is important to note that these patterns include strong peaks for the NiO and YSZ materials in the substrate. In Figure 5, the two control samples, NN0 and LN0, are displayed against the sintered, high-temperature, three-layer NNii sample. The undesirable $Nd_2NiO_4$ can be seen in the red NNii trace primarily at the two split peaks at 32-33 degrees. The control samples only show a single peak at 33 degrees.

Figure 6 shows how all the $NdNiO_3$ samples developed the undesirable $Nd_2NiO_4$ phase upon sintering. The lower temperature of NNiii and NNiv resulted in a more amorphous material than the higher temperature NNii. Figure 7 adds NNv to the same plot. NNv was sintered at ~1040°C, making it somewhat more crystalline than NNiii and NNiv, and more similar to NNii.

Figure 8 shows a blown up view comparing the NN0 control to the single-layer sintered samples NNiii, NNiv, and NNv. The single peak of the NN0 control is evident at 33 degrees, while the sintered samples all show two split peaks at 32-33 degrees, indicating the presence of the undesirable $Nd_2NiO_4$ phase.

Figure 9 indicates the successful maintenance of the desired $LaNiO_3$ phase after sintering for the LNii, LNiii, and LNiv samples. These three patterns are all similar to the LN0 control, with a single peak around 33 degrees. Figure 10 compares LNi and NNii, a lanthanum and neodymium material that both show phase degradation to $(La/Nd)_2NiO_4$.

In summary, $NdNiO_3$ powder (LDRD6), that had about 75% of $NdNiO_3$ phase was sintered at up to 5 different peak temperatures (Utility Global IDs: NNi, Nnii, Nniii, Nniv and NNv) which according to XRD phase analysis resulted in formation of ~60% Nd2NiO4 phase and ~40% $NdNiO_3$ remaining.

$LaNiO_3$ powder (LDRD7) that had about 75-80% of $LaNiO_3$ phase was sintered at up to 4 different peak temperatures (Utility Global IDs: Lni, Lnii, Lniii and Lniv. LNi that was sintered at higher temperatures formed $La_2NiO_4$ ($La_2NiO_4$:$LaNiO_3$ ~50:50), however the other three specimens that were sintered at lower temperatures maintained the $LaNiO_3$ phase (100%) without formation of secondary phases.

Table 4. Summary of XRD phase analysis of LDRD6 LDRD7 from Table 1 after sintering at Utility Global, Inc.

| PNNL sample ID | Utility Global ID | Peak Sintering Temperature (~°C) | XRD after sintering | Comment |
|---|---|---|---|---|
| LDRD 6 | NNi | 1250/950/1050 (three layers) | $Nd_2NiO_4$ + $NdNiO_3$ and $ZrO_2$ + NiO from substrate | Higher degree of amorphous character than NNii |
| LDRD 6 | NNii | 1100/980/1080 (three layers) | $Nd_2NiO_4$ + $NdNiO_3$ and $ZrO_2$ + NiO from substrate | Crystalline. ~60:40 $Nd_2NiO_4$:$NdNiO_3$ |
| LDRD 6 | NNiii | 940 | $Nd_2NiO_4$ + $NdNiO_3$ and $ZrO_2$ + NiO from substrate | Higher degree of amorphous character than NNii |
| LDRD 6 | NNiv | 970 | $Nd_2NiO_4$ + $NdNiO_3$ and $ZrO_2$ + NiO from substrate | Higher degree of amorphous character than NNii |
| LDRD 6 | NNv | 1040 | $Nd_2NiO_4$ + $NdNiO_3$ and $ZrO_2$ + NiO from substrate | More crystalline relative to NNiii and NNiv |
| LDRD 6 | NN0 | Unsintered control | $ZrO_2$ + NiO + $NdNiO_3$ | Substrate YSZ + NiO |
| LDRD 7 | LNi | 1250/1155/1150 (three layers) | $La_2NiO_4$ + $LaNiO_3$ (~50:50) $ZrO_2$ + NiO from substrate | Shows formation of $La_2NiO_4$ after sintering |
| LDRD 7 | LNii | 970 | $LaNiO_3$ $ZrO_2$ + NiO from substrate | Sintered sample similar to LN0 before sintering |
| LDRD 7 | LNiii | 1045 | $LaNiO_3$ $ZrO_2$ + NiO from substrate | Sintered sample similar to LN0 before sintering |
| LDRD 7 | LNiv | 1080 | $LaNiO_3$ $ZrO_2$ + NiO from substrate | Sintered sample similar to LN0 before sintering |
| LDRD 7 | LN0 | Unsintered control | $ZrO_2$ + NiO + $LaNiO_3$ | Substrate YSZ + NiO |

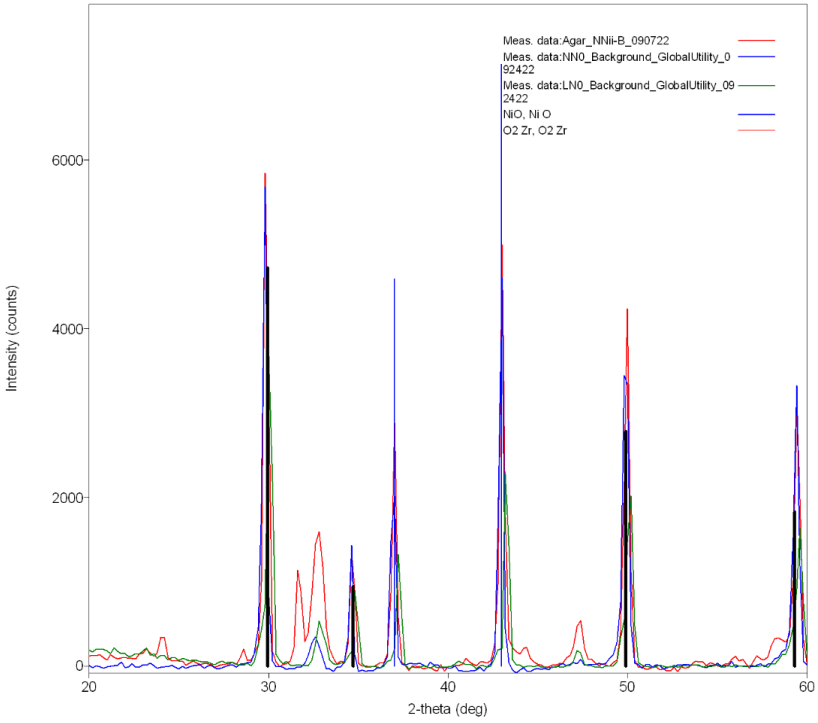


Figure 19. XRD of NN0, substrate + LDRD6 powder before sintering (blue); and LN0, substrate + LDRD7 powder before sintering (green). Phase analysis show $ZrO_2$ + NiO + (Nd/La)$NiO_3$ (black marks). The red pattern is NNii-B which also contains $Nd_2NiO_4$.

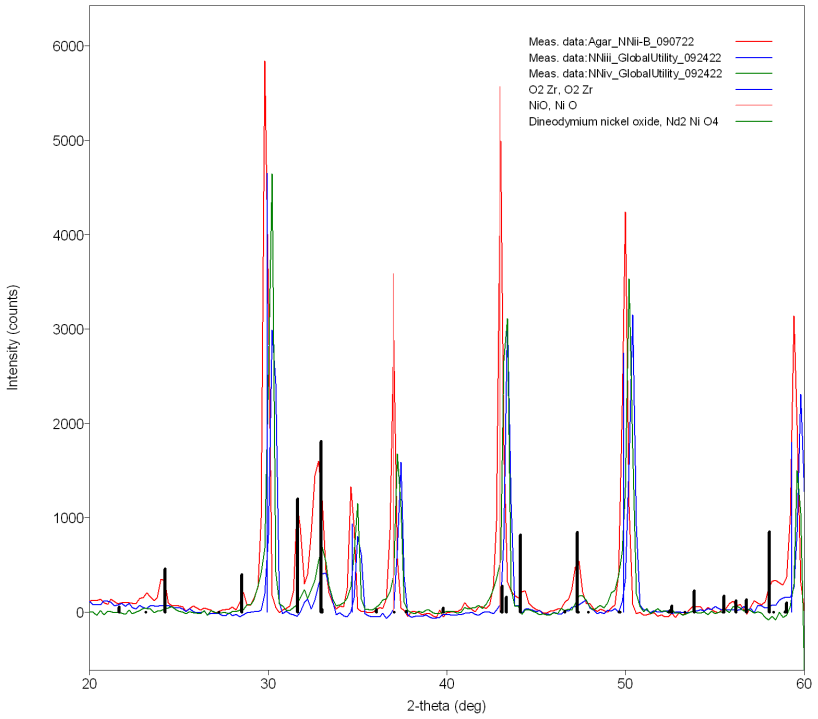


Figure 20. XRD of NNii, NNiii and NNiv after sintering. Phase analysis shows $ZrO_2$ + NiO + $Nd_2NiO_4$ (black marks) + $NdNiO_3$. NNiii and NNiv are more amorphous than NNii.

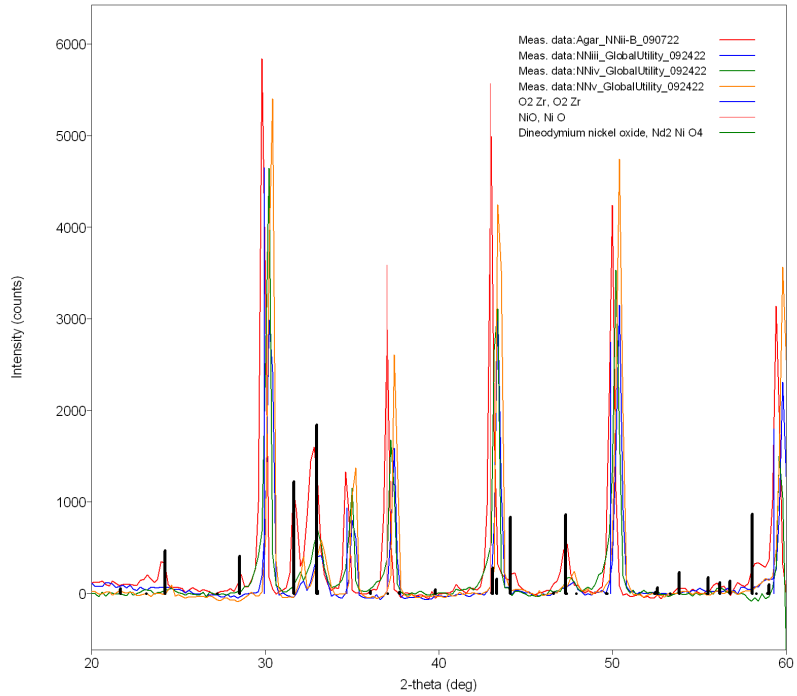


Figure 21. XRD of NNii, NNiii, NNiv and NNv after sintering. Phase analysis shows $ZrO_2$ + NiO + $Nd_2NiO_4$ (black marks) + $NdNiO_3$. NNv is more crystalline than NNiii or NNiv.

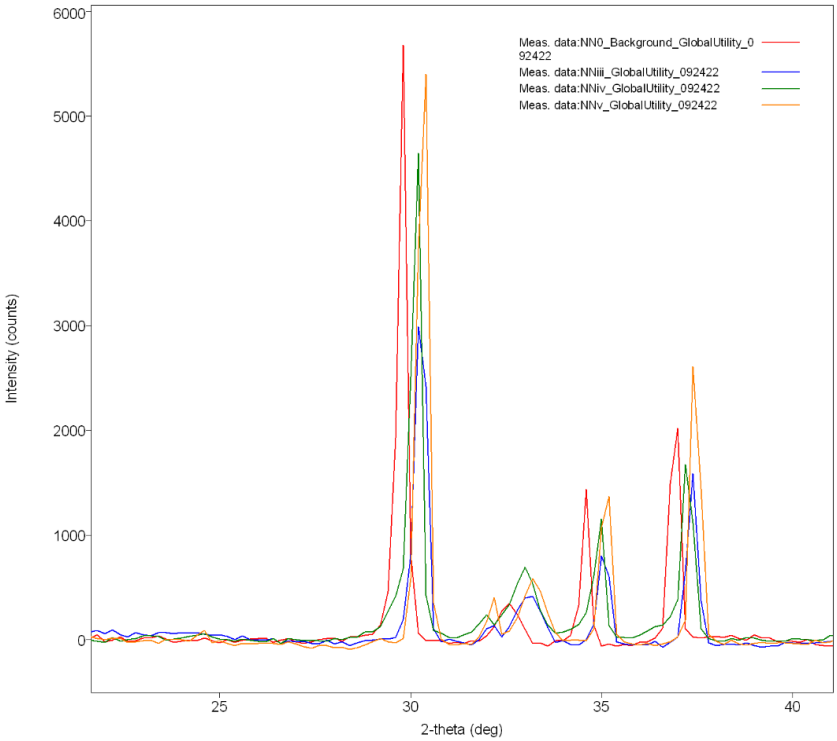


Figure 22. XRD of NN0 (red, unsintered control), and NNiii, NNiv and NNv after sintering. Phase analysis show $ZrO_2$ + NiO + $Nd_2NiO_4$ + $NdNiO_3$ after sintering.

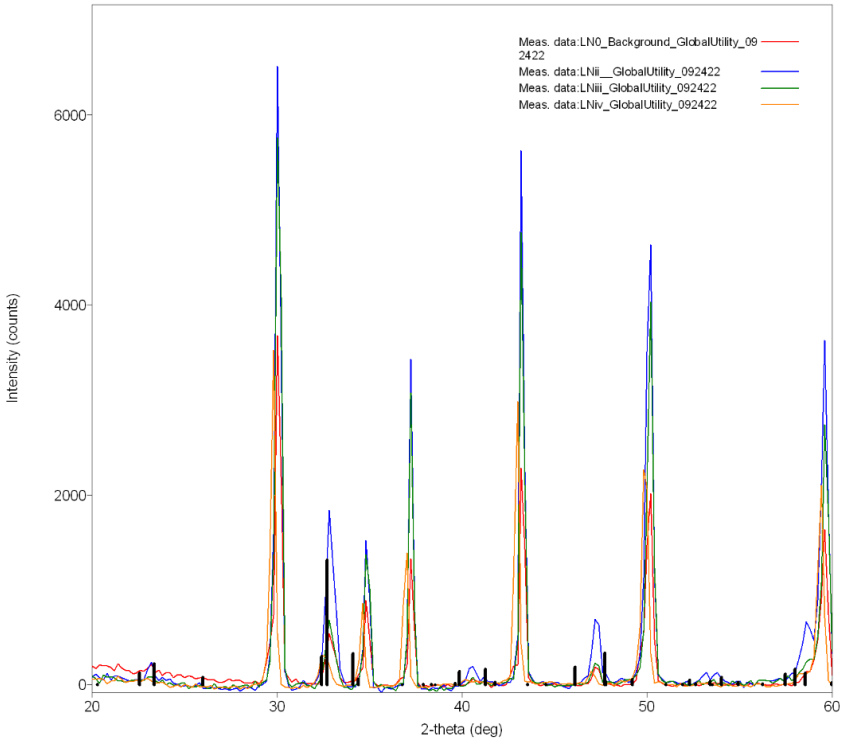


Figure 23. XRD patterns of LN0 (red, unsintered control) and LNii, LNiii, and LNiv after sintering. The phase analysis shows $ZrO_2$ + NiO + $LaNiO_3$ (black marks) before and after sintering.

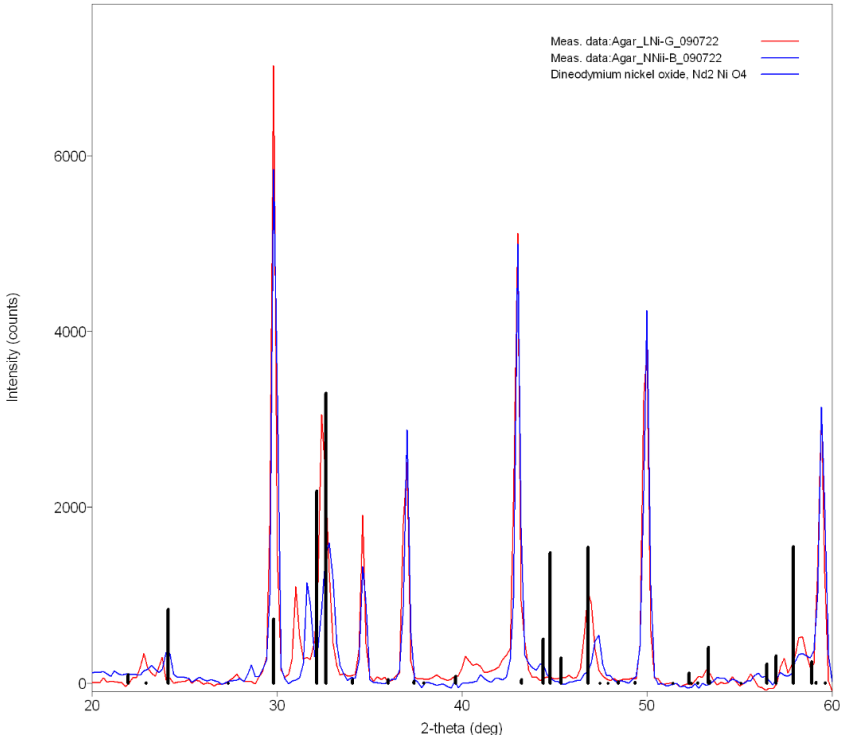


Figure 24. XRD of LNi (red) and NNii (blue). Phase analysis shows $ZrO_2$ + NiO + $(Nd/La)_2NiO_4$ + $(Nd/La)NiO_3$ after sintering. Black markers indicate $Nd_2NiO_4$ phase.

# 5.0 Conclusions

The proton conducting lanthanide nickelates, $LaNiO_3$ and $NdNiO_3$, were synthesized at 75-80% purity via a facile precursor solid solution method utilizing bleach as the oxidizing agent. Both powders were sintered at Utility Global Inc. at various temperatures utilizing fast photonic sintering. Single layers of $LaNiO_3$ were successfully sintered while maintaining the perovskite phase. Single layers of $NdNiO_3$ underwent a phase transformation at all the conditions tested. The stability of the perovskite phase decreases moving right across the lanthanides in the periodic table, while the expected proton conductivity increases. These results will inform further investigations into lanthanide nickelate perovskites toward the goal of producing a free-standing, sintered, proton-conducting membrane.

# 6.0 References

Chick, L. A., L. R. Pederson, G. D. Maupin, J. L. Bates, L. E. Thomas, G. J. Exarhos, Glycine-nitrate combustion synthesis of oxide ceramic powders, Mater. Letters, 10 (1990) 6-12.

Le, Ngo Thi Hong, José M. Calderón-Moreno, Mónica Popa, Daniel Crespo, Le Van Hong, Nguyen Xuan Phuc, $LaNiO_3$ Nanopowder Prepared by an “Amorphous Citrate” Route, J. Eur. Ceram. Soc., 26 (2006) 403-407.

Oliveira F. S., P. M. Pimentel, R. M. P. B. Oliveira, D. M. A. Melo, M. A. F. Melo, Effect of Lanthanum Replacement By Strontium in Lanthanum Nickelate Crystals Synthesized Using Gelatin as Organic Precursor, Materials Letters, 64 (2010) 2700-2703.

Oliveira, R. M. P. B., P. M. Pimentel, J. H. Araújo, D. M. S. Melo, M. A. F. Melo, E. E. Martinelli, Microstructural Study of Neodymium Nickelate Doped with Strontium Synthesized by Gelatin Method, Advances in Materials Science and Engineering, Vol. 2013, Article 926540

Vidyasagar, K., J. Gopalakrishnan, C. N. R. Rao, Synthesis of Complex Metal Oxides Using Hydroxide, Cyanide, and Nitrate Solid Solution Precursors, J. Solid State Chem., 58 (1985) 29-37.

# Pacific Northwest National Laboratory

902 Battelle Boulevard
P.O. Box 999
Richland, WA 99354

1-888-375-PNNL (7665)

***www.pnnl.gov***